Search for Production of Invisible Final States in Single-Photon Decays of $\Upsilon(1S)$

P. del Amo Sanchez,[1] J. P. Lees,[1] V. Poireau,[1] E. Prencipe,[1] V. Tisserand,[1] J. Garra Tico,[2] E. Grauges,[2] M. Martinelli,[3a,3b] D. A. Milanes,[3a,3b] A. Palano,[3a,3b] M. Pappagallo,[3a,3b] G. Eigen,[4] B. Stugu,[4] L. Sun,[4] D. N. Brown,[5] M. V. Chistiakova,[5] F. Jensen,[5] L. T. Kerth,[5] Yu. G. Kolomensky,[5] G. Lynch,[5] I. L. Osipenkov,[5] H. Koch,[6] T. Schroeder,[6] D. J. Asgeirsson,[7] C. Hearty,[7] T. S. Mattison,[7] J. A. McKenna,[7] A. Khan,[8] A. Randle-Conde,[8] V. E. Blinov,[9] A. R. Buzykaev,[9] V. P. Druzhinin,[9] V. B. Golubev,[9] E. A. Kravchenko,[9] A. P. Onuchin,[9] S. I. Serednyakov,[9] Yu. I. Skovpen,[9] E. P. Solodov,[9] K. Yu. Todyshev,[9] A. N. Yushkov,[9] M. Bondioli,[10] S. Curry,[10] D. Kirkby,[10] A. J. Lankford,[10] M. Mandelkern,[10] E. C. Martin,[10] D. P. Stoker,[10] H. Atmacan,[11] J. W. Gary,[11] F. Liu,[11] O. Long,[11] G. M. Vitug,[11] C. Campagnari,[12] T. M. Hong,[12] D. Kovalskyi,[12] J. D. Richman,[12] C. West,[12] A. M. Eisner,[13] C. A. Heusch,[13] J. Kroseberg,[13] W. S. Lockman,[13] A. J. Martinez,[13] T. Schalk,[13] B. A. Schumm,[13] A. Seiden,[13] L. O. Winstrom,[13] C. H. Cheng,[14] D. A. Doll,[14] B. Echenard,[14] D. G. Hitlin,[14] P. Ongmongkolkul,[14] F. C. Porter,[14] A. Y. Rakitin,[14] R. Andreassen,[15] M. S. Dubrovin,[15] G. Mancinelli,[15] B. T. Meadows,[15] M. D. Sokoloff,[15] P. C. Bloom,[16] W. T. Ford,[16] A. Gaz,[16] M. Nagel,[16] U. Nauenberg,[16] J. G. Smith,[16] S. R. Wagner,[16] R. Ayad,[17,*] W. H. Toki,[17] H. Jasper,[18] T. M. Karbach,[18] A. Petzold,[18] B. Spaan,[18] M. J. Kobel,[19] K. R. Schubert,[19] R. Schwierz,[19] D. Bernard,[20] M. Verderi,[20] P. J. Clark,[21] S. Playfer,[21] J. E. Watson,[21] M. Andreotti,[22a,22b] D. Bettoni,[22a] C. Bozzi,[22a] R. Calabrese,[22a,22b] A. Cecchi,[22a,22b] G. Cibinetto,[22a,22b] E. Fioravanti,[22a,22b] P. Franchini,[22a,22b] I. Garzia,[22a,22b] E. Luppi,[22a,22b] M. Munerato,[22a,22b] M. Negrini,[22a,22b] A. Petrella,[22a,22b] L. Piemontese,[22a,22b] R. Baldini-Ferroli,[23] A. Calcaterra,[23] R. de Sangro,[23] G. Finocchiaro,[23] M. Nicolaci,[23] S. Pacetti,[23] P. Patteri,[23] I. M. Peruzzi,[23,†] M. Piccolo,[23] M. Rama,[23] A. Zallo,[23] R. Contri,[24a,24b] E. Guido,[24a,24b] M. Lo Vetere,[24a,24b] M. R. Monge,[24a,24b] S. Passaggio,[24a] C. Patrignani,[24a,24b] E. Robutti,[24a] S. Tosi,[24a,24b] B. Bhuyan,[25] V. Prasad,[25] C. L. Lee,[26] M. Morii,[26] A. Adametz,[27] J. Marks,[27] U. Uwer,[27] F. U. Bernlochner,[28] M. Ebert,[28] H. M. Lacker,[28] T. Lueck,[28] A. Volk,[28] P. D. Dauncey,[29] M. Tibbetts,[29] P. K. Behera,[30] U. Mallik,[30] C. Chen,[31] J. Cochran,[31] H. B. Crawley,[31] L. Dong,[31] W. T. Meyer,[31] S. Prell,[31] E. I. Rosenberg,[31] A. E. Rubin,[31] A. V. Gritsan,[32] Z. J. Guo,[32] N. Arnaud,[33] M. Davier,[33] D. Derkach,[33] J. Firmino da Costa,[33] G. Grosdidier,[33] F. Le Diberder,[33] A. M. Lutz,[33] B. Malaescu,[33] A. Perez,[33] P. Roudeau,[33] M. H. Schune,[33] J. Serrano,[33] V. Sordini,[33,‡] A. Stocchi,[33] L. Wang,[33] G. Wormser,[33] D. J. Lange,[34] D. M. Wright,[34] I. Bingham,[35] C. A. Chavez,[35] J. P. Coleman,[35] J. R. Fry,[35] E. Gabathuler,[35] R. Gamet,[35] D. E. Hutchcroft,[35] D. J. Payne,[35] C. Touramanis,[35] A. J. Bevan,[36] F. Di Lodovico,[33] R. Sacco,[36] M. Sigamani,[36] G. Cowan,[37] S. Paramesvaran,[37] A. C. Wren,[37] D. N. Brown,[38] C. L. Davis,[38] A. G. Denig,[39] M. Fritsch,[39] W. Gradl,[39] A. Hafner,[39] K. E. Alwyn,[40] D. Bailey,[40] R. J. Barlow,[40] G. Jackson,[40] G. D. Lafferty,[40] J. Anderson,[41] R. Cenci,[41] A. Jawahery,[41] D. A. Roberts,[41] G. Simi,[41] J. M. Tuggle,[41] C. Dallapiccola,[42] E. Salvati,[42] R. Cowan,[43] D. Dujmic,[43] G. Sciolla,[43] M. Zhao,[43] D. Lindemann,[44] P. M. Patel,[44] S. H. Robertson,[44] M. Schram,[44] P. Biassoni,[45a,45b] A. Lazzaro,[45a,45b] V. Lombardo,[45a] F. Palombo,[45a,45b] S. Stracka,[45a,45b] L. Cremaldi,[46] R. Godang,[46,§] R. Kroeger,[46] P. Sonnek,[46] D. J. Summers,[46] X. Nguyen,[47] M. Simard,[47] P. Taras,[47] G. De Nardo,[48a,48b] D. Monorchio,[48a,48b] G. Onorato,[48a,48b] C. Sciacca,[48a,48b] G. Raven,[49] H. L. Snoek,[49] C. P. Jessop,[50] K. J. Knoepfel,[50] J. M. LoSecco,[50] W. F. Wang,[50] L. A. Corwin,[51] K. Honscheid,[51] R. Kass,[51] J. P. Morris,[51] N. L. Blount,[52] J. Brau,[52] R. Frey,[52] O. Igonkina,[52] J. A. Kolb,[52] R. Rahmat,[52] N. B. Sinev,[52] D. Strom,[52] J. Strube,[52] E. Torrence,[52] G. Castelli,[53a,53b] E. Feltresi,[53a,53b] N. Gagliardi,[53a,53b] M. Margoni,[53a,53b] M. Morandin,[53a] M. Posocco,[53a] M. Rotondo,[53a] F. Simonetto,[53a,53b] R. Stroili,[53a,53b] E. Ben-Haim,[54] G. R. Bonneaud,[54] H. Briand,[54] G. Calderini,[54] J. Chauveau,[54] O. Hamon,[54] Ph. Leruste,[54] G. Marchiori,[54] J. Ocariz,[54] J. Prendki,[54] S. Sitt,[54] M. Biasini,[55a,55b] E. Manoni,[55a,55b] A. Rossi,[55a,55b] C. Angelini,[56a,56b] G. Batignani,[56a,56b] S. Bettarini,[56a,56b] M. Carpinelli,[56a,56b,‖] G. Casarosa,[56a,56b] A. Cervelli,[56a,56b] F. Forti,[56a,56b] M. A. Giorgi,[56a,56b] A. Lusiani,[56a,56c] N. Neri,[56a,56b] E. Paoloni,[56a,56b] G. Rizzo,[56a,56b] J. J. Walsh,[56a] D. Lopes Pegna,[57] C. Lu,[57] J. Olsen,[57] A. J. S. Smith,[57] A. V. Telnov,[57] F. Anulli,[58a] E. Baracchini,[58a,58b] G. Cavoto,[58a] R. Faccini,[58a,58b] F. Ferrarotto,[58a] F. Ferroni,[58a,58b] M. Gaspero,[58a,58b] L. Li Gioi,[58a] M. A. Mazzoni,[58a] G. Piredda,[58a] F. Renga,[58a,58b] T. Hartmann,[59] T. Leddig,[59] H. Schröder,[59] R. Waldi,[59] T. Adye,[60] B. Franek,[60] E. O. Olaiya,[60] F. F. Wilson,[60] S. Emery,[61] G. Hamel de Monchenault,[61] G. Vasseur,[61] Ch. Yèche,[61] M. Zito,[61] M. T. Allen,[62] D. Aston,[62] D. J. Bard,[62] R. Bartoldus,[62] J. F. Benitez,[62] C. Cartaro,[62] M. R. Convery,[62] J. Dorfan,[62] G. P. Dubois-Felsmann,[62] W. Dunwoodie,[62] R. C. Field,[62] M. Franco Sevilla,[62] B. G. Fulsom,[62] A. M. Gabareen,[62] M. T. Graham,[62] P. Grenier,[62] C. Hast,[62] W. R. Innes,[62] M. H. Kelsey,[62] H. Kim,[62] P. Kim,[62] M. L. Kocian,[62] D. W. G. S. Leith,[62] S. Li,[62] B. Lindquist,[62] S. Luitz,[62] V. Luth,[62] H. L. Lynch,[62] D. B. MacFarlane,[62] H. Marsiske,[62] D. R. Muller,[62] H. Neal,[62] S. Nelson,[62] C. P. O'Grady,[62] I. Ofte,[62] M. Perl,[62] T. Pulliam,[62] B. N. Ratcliff,[62] A. Roodman,[62] A. A. Salnikov,[62] V. Santoro,[62] R. H. Schindler,[62] J. Schwiening,[62]

A. Snyder,[62] D. Su,[62] M. K. Sullivan,[62] S. Sun,[62] K. Suzuki,[62] J. M. Thompson,[62] J. Va'vra,[62] A. P. Wagner,[62] M. Weaver,[62] W. J. Wisniewski,[62] M. Wittgen,[62] D. H. Wright,[62] H. W. Wulsin,[62] A. K. Yarritu,[62] C. C. Young,[62] V. Ziegler,[62] X. R. Chen,[63] W. Park,[63] M. V. Purohit,[63] R. M. White,[63] J. R. Wilson,[63] S. J. Sekula,[64] M. Bellis,[65] P. R. Burchat,[65] A. J. Edwards,[65] T. S. Miyashita,[65] S. Ahmed,[66] M. S. Alam,[66] J. A. Ernst,[66] B. Pan,[66] M. A. Saeed,[66] S. B. Zain,[66] N. Guttman,[67] A. Soffer,[67] P. Lund,[68] S. M. Spanier,[68] R. Eckmann,[69] J. L. Ritchie,[69] A. M. Ruland,[69] C. J. Schilling,[69] R. F. Schwitters,[69] B. C. Wray,[69] J. M. Izen,[70] X. C. Lou,[70] F. Bianchi,[71a,71b] D. Gamba,[71a,71b] M. Pelliccioni,[71a,71b] M. Bomben,[72a,72b] L. Lanceri,[72a,72b] L. Vitale,[72a,72b] N. Lopez-March,[73] F. Martinez-Vidal,[73] A. Oyanguren,[73] J. Albert,[74] Sw. Banerjee,[74] H. H. F. Choi,[74] K. Hamano,[74] G. J. King,[74] R. Kowalewski,[74] M. J. Lewczuk,[74] C. Lindsay,[74] I. M. Nugent,[74] J. M. Roney,[74] R. J. Sobie,[74] T. J. Gershon,[75] P. F. Harrison,[75] T. E. Latham,[75] E. M. T. Puccio,[75] H. R. Band,[76] S. Dasu,[76] K. T. Flood,[76] Y. Pan,[76] R. Prepost,[76] C. O. Vuosalo,[76] and S. L. Wu[76]

(*BABAR* Collaboration)

[1]*Laboratoire d'Annecy-le-Vieux de Physique des Particules (LAPP), Université de Savoie, CNRS/IN2P3, F-74941 Annecy-Le-Vieux, France*
[2]*Universitat de Barcelona, Facultat de Fisica, Departament ECM, E-08028 Barcelona, Spain*
[3a]*INFN Sezione di Bari, I-70126 Bari, Italy*
[3b]*Dipartimento di Fisica, Università di Bari, I-70126 Bari, Italy*
[4]*University of Bergen, Institute of Physics, N-5007 Bergen, Norway*
[5]*Lawrence Berkeley National Laboratory and University of California, Berkeley, California 94720, USA*
[6]*Ruhr Universität Bochum, Institut für Experimentalphysik 1, D-44780 Bochum, Germany*
[7]*University of British Columbia, Vancouver, British Columbia, Canada V6T 1Z1*
[8]*Brunel University, Uxbridge, Middlesex UB8 3PH, United Kingdom*
[9]*Budker Institute of Nuclear Physics, Novosibirsk 630090, Russia*
[10]*University of California at Irvine, Irvine, California 92697, USA*
[11]*University of California at Riverside, Riverside, California 92521, USA*
[12]*University of California at Santa Barbara, Santa Barbara, California 93106, USA*
[13]*University of California at Santa Cruz, Institute for Particle Physics, Santa Cruz, California 95064, USA*
[14]*California Institute of Technology, Pasadena, California 91125, USA*
[15]*University of Cincinnati, Cincinnati, Ohio 45221, USA*
[16]*University of Colorado, Boulder, Colorado 80309, USA*
[17]*Colorado State University, Fort Collins, Colorado 80523, USA*
[18]*Technische Universität Dortmund, Fakultät Physik, D-44221 Dortmund, Germany*
[19]*Technische Universität Dresden, Institut für Kern-und Teilchenphysik, D-01062 Dresden, Germany*
[20]*Laboratoire Leprince-Ringuet, CNRS/IN2P3, Ecole Polytechnique, F-91128 Palaiseau, France*
[21]*University of Edinburgh, Edinburgh EH9 3JZ, United Kingdom*
[22a]*INFN Sezione di Ferrara, I-44100 Ferrara, Italy*
[22b]*Dipartimento di Fisica, Università di Ferrara, I-44100 Ferrara, Italy*
[23]*INFN Laboratori Nazionali di Frascati, I-00044 Frascati, Italy*
[24a]*INFN Sezione di Genova, I-16146 Genova, Italy*
[24b]*Dipartimento di Fisica, Università di Genova, I-16146 Genova, Italy*
[25]*Indian Institute of Technology Guwahati, Guwahati, Assam, 781 039, India*
[26]*Harvard University, Cambridge, Massachusetts 02138, USA*
[27]*Universität Heidelberg, Physikalisches Institut, Philosophenweg 12, D-69120 Heidelberg, Germany*
[28]*Humboldt-Universität zu Berlin, Institut für Physik, Newtonstraße 15, D-12489 Berlin, Germany*
[29]*Imperial College London, London, SW7 2AZ, United Kingdom*
[30]*University of Iowa, Iowa City, Iowa 52242, USA*
[31]*Iowa State University, Ames, Iowa 50011-3160, USA*
[32]*Johns Hopkins University, Baltimore, Maryland 21218, USA*
[33]*Laboratoire de l'Accélérateur Linéaire, IN2P3/CNRS et Université Paris-Sud 11, Centre Scientifique d'Orsay, Boîte Postale 34, F-91898 Orsay Cedex, France*
[34]*Lawrence Livermore National Laboratory, Livermore, California 94550, USA*
[35]*University of Liverpool, Liverpool L69 7ZE, United Kingdom*
[36]*Queen Mary, University of London, London, E1 4NS, United Kingdom*
[37]*University of London, Royal Holloway and Bedford New College, Egham, Surrey TW20 0EX, United Kingdom*
[38]*University of Louisville, Louisville, Kentucky 40292, USA*
[39]*Johannes Gutenberg-Universität Mainz, Institut für Kernphysik, D-55099 Mainz, Germany*
[40]*University of Manchester, Manchester M13 9PL, United Kingdom*

[41]University of Maryland, College Park, Maryland 20742, USA
[42]University of Massachusetts, Amherst, Massachusetts 01003, USA
[43]Massachusetts Institute of Technology, Laboratory for Nuclear Science, Cambridge, Massachusetts 02139, USA
[44]McGill University, Montréal, Québec, Canada H3A 2T8
[45a]INFN Sezione di Milano, I-20133 Milano, Italy
[45b]Dipartimento di Fisica, Università di Milano, I-20133 Milano, Italy
[46]University of Mississippi, University, Mississippi 38677, USA
[47]Université de Montréal, Physique des Particules, Montréal, Québec, Canada H3C 3J7
[48a]INFN Sezione di Napoli, I-80126 Napoli, Italy
[48b]Dipartimento di Scienze Fisiche, Università di Napoli Federico II, I-80126 Napoli, Italy
[49]NIKHEF, National Institute for Nuclear Physics and High Energy Physics, NL-1009 DB Amsterdam, The Netherlands
[50]University of Notre Dame, Notre Dame, Indiana 46556, USA
[51]Ohio State University, Columbus, Ohio 43210, USA
[52]University of Oregon, Eugene, Oregon 97403, USA
[53a]INFN Sezione di Padova, I-35131 Padova, Italy
[53b]Dipartimento di Fisica, Università di Padova, I-80126 Napoli, Italy
[54]Laboratoire de Physique Nucléaire et de Hautes Energies, IN2P3/CNRS, Université Pierre et Marie Curie-Paris6, Université Denis Diderot-Paris7, F-75252 Paris, France
[55a]INFN Sezione di Perugia, I-06100 Perugia, Italy
[55b]Dipartimento di Fisica, Università di Perugia, I-06100 Perugia, Italy
[56a]INFN Sezione di Pisa, I-56127 Pisa, Italy
[56b]Dipartimento di Fisica, Università di Pisa, I-56127 Pisa, Italy
[56c]Scuola Normale Superiore di Pisa, I-56127 Pisa, Italy
[57]Princeton University, Princeton, New Jersey 08544, USA
[58a]INFN Sezione di Roma, I-00185 Roma, Italy
[58b]Dipartimento di Fisica, Università di Roma La Sapienza, I-00185 Roma, Italy
[59]Universität Rostock, D-18051 Rostock, Germany
[60]Rutherford Appleton Laboratory, Chilton, Didcot, Oxon, OX11 0QX, United Kingdom
[61]CEA, Irfu, SPP, Centre de Saclay, F-91191 Gif-sur-Yvette, France
[62]SLAC National Accelerator Laboratory, Stanford, California 94309 USA
[63]University of South Carolina, Columbia, South Carolina 29208, USA
[64]Southern Methodist University, Dallas, Texas 75275, USA
[65]Stanford University, Stanford, California 94305-4060, USA
[66]State University of New York, Albany, New York 12222, USA
[67]Tel Aviv University, School of Physics and Astronomy, Tel Aviv, 69978, Israel
[68]University of Tennessee, Knoxville, Tennessee 37996, USA
[69]University of Texas at Austin, Austin, Texas 78712, USA
[70]University of Texas at Dallas, Richardson, Texas 75083, USA
[71a]INFN Sezione di Torino, I-10125 Torino, Italy
[71b]Dipartimento di Fisica Sperimentale, Università di Torino, I-10125 Torino, Italy
[72a]INFN Sezione di Trieste, I-34127 Trieste, Italy
[72b]Dipartimento di Fisica, Università di Trieste, I-34127 Trieste, Italy
[73]IFIC, Universitat de Valencia-CSIC, E-46071 Valencia, Spain
[74]University of Victoria, Victoria, British Columbia, Canada V8W 3P6
[75]Department of Physics, University of Warwick, Coventry CV4 7AL, United Kingdom
[76]University of Wisconsin, Madison, Wisconsin 53706, USA

(Received 26 July 2010; published 6 July 2011)

We search for single-photon decays of the $\Upsilon(1S)$ resonance, $\Upsilon \to \gamma +$ invisible, where the invisible state is either a particle of definite mass, such as a light Higgs boson A^0, or a pair of dark matter particles, $\chi\bar{\chi}$. Both A^0 and χ are assumed to have zero spin. We tag $\Upsilon(1S)$ decays with a dipion transition $\Upsilon(2S) \to \pi^+\pi^-\Upsilon(1S)$ and look for events with a single energetic photon and significant missing energy. We find no evidence for such processes in the mass range $m_{A^0} \leq 9.2$ GeV and $m_\chi \leq 4.5$ GeV in the sample of 98×10^6 $\Upsilon(2S)$ decays collected with the *BABAR* detector and set stringent limits on new physics models that contain light dark matter states.

DOI: 10.1103/PhysRevLett.107.021804 PACS numbers: 13.20.Gd, 12.60.Jv, 14.80.Da, 95.35.+d

There is compelling astrophysical evidence for the existence of dark matter [1,2], which amounts to about one-quarter of the total energy density in the Universe. Yet there is no experimental information on the particle

composition of dark matter [2,3]. A class of new physics models [4], motivated by astroparticle observations [5,6], predicts a light component of the dark matter spectrum. The bottomonium system of Υ states is an ideal environment to explore these models. Transitions $\Upsilon(3S) \to \pi^+\pi^-\Upsilon(1S)$ and $\Upsilon(2S) \to \pi^+\pi^-\Upsilon(1S)$ offer a way to cleanly detect the production of $\Upsilon(1S)$ mesons, and enable searches for invisible or nearly invisible decays of the $\Upsilon(1S)$ [7]. Such decays would be a telltale sign of low-mass, weakly interacting dark matter particles.

The standard model process $\Upsilon(1S) \to \gamma\nu\bar{\nu}$ is not observable at the present experimental sensitivity [8]. An observation of Υ decays with significant missing energy would be a sign of new physics, and could shed light on the spectrum of dark matter particles χ. The branching fraction (BF) $\mathcal{B}(\Upsilon(1S) \to \chi\bar{\chi})$ is estimated to be as large as $(4\text{–}18) \times 10^{-4}$ [8,9], while $\mathcal{B}(\Upsilon(1S) \to \gamma\chi\bar{\chi})$ is suppressed by $\mathcal{O}(\alpha)$, and the range 10^{-5}–10^{-4} is expected [8].

The decays $\Upsilon(1S) \to \gamma$ + invisible might also proceed through Wilczek production [10] of an on-shell scalar state A^0: $\Upsilon(1S) \to \gamma A^0$, $A^0 \to$ invisible. Such low-mass Higgs states appear in several extensions of the standard model [11]. Constraining the low-mass Higgs sector is important for understanding the Higgs discovery reach of high-energy colliders [12]. The BF for $\Upsilon(1S) \to \gamma A^0$ is predicted to be as large as 5×10^{-4}, depending on m_{A^0} and couplings [13]. If there is also a low-mass neutralino with mass $m_\chi < m_{A^0}/2$, the decays of A^0 would be predominantly invisible [14].

For multibody $\Upsilon(1S) \to \gamma\chi\bar{\chi}$ decays, the current 90% confidence level (C.L.) BF upper limit, based on a data sample of $\sim 10^6$ $\Upsilon(1S)$ decays, is of order 10^{-3} [15]. The limit on two-body $\Upsilon(1S) \to \gamma + X$, $X \to$ invisible decays is $\mathcal{B}(\Upsilon(1S) \to \gamma + X) < 3 \times 10^{-5}$ for $m_X < 7.2$ GeV [3]. The limit on invisible decays of $\Upsilon(1S)$ is $\mathcal{B}(\Upsilon(1S) \to \chi\bar{\chi}) < 3.0 \times 10^{-4}$ [7].

This Letter describes a high-statistics, low-background search for decays $\Upsilon(1S) \to \gamma$ + invisible, characterized by a single energetic photon and a large amount of missing energy and momentum. This is the first search of this kind to use the $\Upsilon(1S)$ mesons produced in dipion $\Upsilon(2S) \to \pi^+\pi^-\Upsilon(1S)$ transitions. We search for both resonant two-body decays $\Upsilon(1S) \to \gamma A^0$, $A^0 \to$ invisible, and nonresonant three-body processes $\Upsilon(1S) \to \gamma\chi\bar{\chi}$. For the resonant process, we assume that the decay width of the A^0 resonance is negligible compared to the experimental resolution [16]. We further assume that both the A^0 and χ particles have zero spin. The decays $\Upsilon(1S) \to \gamma\chi\bar{\chi}$ are modeled with phase-space energy and angular distributions, which corresponds to S-wave coupling between the $b\bar{b}$ and $\chi\bar{\chi}$.

The analysis is based on a sample corresponding to an integrated luminosity of 14.4 fb^{-1} collected on the $\Upsilon(2S)$ resonance with the *BABAR* detector at the PEP-II asymmetric-energy e^+e^- collider at the SLAC National Accelerator Laboratory. This sample corresponds to $(98.3 \pm 0.9) \times 10^6$ $\Upsilon(2S)$ decays. We also employ a sample of 28 fb^{-1} accumulated on the $\Upsilon(3S)$ resonance [$\Upsilon(3S)$ sample] for studies of the continuum backgrounds. Both $\Upsilon(3S) \to \pi^+\pi^-\Upsilon(2S)$ and $\Upsilon(3S) \to \pi^+\pi^-\Upsilon(1S)$ decays produce a dipion system that is kinematically distinct from the $\Upsilon(2S) \to \pi^+\pi^-\Upsilon(1S)$ transition. Hence, the $\Upsilon(3S)$ events passing our selection form a pure high-statistics continuum QED sample. For selection optimization, we also use 1.4 fb^{-1} and 2.4 fb^{-1} data sets collected about 30 MeV below the $\Upsilon(2S)$ and $\Upsilon(3S)$ resonances, respectively (off-peak samples). The *BABAR* detector, including the tracking and particle identification systems, the electromagnetic calorimeter (EMC), and the instrumented flux return (IFR), is described in detail elsewhere [17,18].

Detection of low-multiplicity events requires dedicated trigger and filter lines. First, the hardware-based level-1 (L1) trigger accepts single-photon events if they contain at least one EMC cluster with energy above 800 MeV. A collection of L1 trigger patterns based on drift chamber information selects a pair of low-momentum pions. Second, a software-based level-3 (L3) trigger accepts events with a single EMC cluster with the center-of-mass (c.m.) energy $E^*_\gamma > 1$ GeV [19], if there is no charged track with transverse momentum $p_T > 0.25$ GeV originating from the e^+e^- interaction region. Complementary to this, a track-based L3 trigger accepts events that have at least one track with $p_T > 0.2$ GeV. Third, an offline filter accepts events that have exactly one photon with energy $E^*_\gamma > 1$ GeV, and no tracks with momentum $p^* > 0.5$ GeV. A nearly independent filter accepts events with two tracks of opposite charge, which form a dipion candidate with recoil mass (defined below) between 9.35 and 9.60 GeV.

The analysis in the low-mass region $m_{A^0} \leq 8$ GeV ($m_\chi \leq 4$ GeV), which corresponds to photon energies $E^*_\gamma > 1.1$ GeV, requires the single-photon or the dipion trigger or filter selection to be satisfied; the trigger or filter efficiency for the signal is 83%. In the high-mass region, $7.5 \leq m_{A^0} \leq 9.2$ GeV ($3.5 \leq m_\chi \leq 4.5$ GeV), we only accept events selected with the dipion trigger or filter, since a significant fraction of this region lies below the energy threshold for the single-photon selection. This selection has an efficiency of 12.5% for signal events.

We select events with exactly two oppositely charged tracks and a single energetic photon with $E^*_\gamma \geq 0.15$ GeV in the central part of the EMC ($-0.73 < \cos\theta^*_\gamma < 0.68$). Additional photons with $E^*_\gamma \leq 0.12$ GeV can be present so long as their summed laboratory energy is less than 0.14 GeV. We require that both pions be positively identified with 85%–98% efficiency for real pions, and a misidentification rate of $<5\%$ for low-momentum electrons and $<1\%$ for kaons and protons. The pion candidates are required to form a vertex with $\chi^2_{\rm vtx} < 20$ (1 degree of freedom) displaced in the transverse plane by at most

2 mm from the e^+e^- interaction region. The transverse momentum of the pion pair is required to satisfy $p_{T\pi\pi} < 0.5$ GeV, and we reject events if any track has $p^* > 1$ GeV.

We further reduce the background by combining several kinematic variables of the dipion system [7] into a multilayer perceptron neural network discriminant (NN) [20]. The NN is trained with a sample of simulated signal events $\Upsilon(1S) \to \gamma\chi\bar{\chi}$ ($m_\chi = 0$) and an off-peak sample for background; the NN assigns a value $\mathcal{N}$ close to $+1$ for signal and close to -1 for background. We require $\mathcal{N} > 0.65$ in the low-mass region. This selection has an efficiency of 87% for signal and rejects 96% of the continuum background. In the high-mass region we require $\mathcal{N} > 0.89$ (73% signal efficiency, 98% continuum rejection).

Two additional requirements are applied to reduce specific background contributions. Neutral hadrons from the radiative decays $\Upsilon(1S) \to \gamma K_L^0 K_L^0$ and $\Upsilon(1S) \to \gamma n\bar{n}$ may not be detected in the EMC. We remove 90% of these background events by requiring that there be no IFR cluster within a range of 20° of azimuthal angle (ϕ) opposite the primary photon (IFR veto). This selection is applied for $m_{A^0} < 4$ GeV and $m_\chi < 2$ GeV, since the hadronic final states in radiative $\Upsilon(1S)$ decays are observed to have low invariant mass [21].

For the high-mass range we suppress contamination from electron bremsstrahlung by rejecting events if the photon and one of the tracks are closer than 14° in ϕ. In addition, the two-photon process $e^+e^- \to e^+e^-\gamma^*\gamma^* \to e^+e^-\eta'$, $\eta' \to \gamma\pi^+\pi^-$, in which the e^+e^- pair escapes detection along the beam axis and the two pions satisfy our selection criteria, produces photons in a narrow energy range $0.25 < E_\gamma^* < 0.45$ GeV. We take advantage of the small transverse momentum of the η' and reject over half of these events by requiring the primary photon and dipion system to be separated by at most $\Delta\phi = 160°$. The signal efficiency for this requirement is 88%.

The selection criteria are chosen to maximize $\varepsilon/(1.5 + \sqrt{B})$ [22], where ε is the selection efficiency for $m_\chi = 0$ and B is the expected background yield. The signal efficiency varies between 2% and 11%, and is lowest at the highest masses (lowest photon energy). The backgrounds can be classified into three categories: continuum backgrounds from QED processes $e^+e^- \to \gamma\pi^+\pi^- + \ldots$ with particles escaping detection, radiative leptonic decays $\Upsilon(1S) \to \gamma\ell^+\ell^-$, where leptons $\ell \equiv e$, μ, τ are not detected, and peaking backgrounds from radiative hadronic decays and two-photon η' production.

We extract the yield of signal events as a function of m_{A^0} (m_χ) in the interval $0 \le m_{A^0} \le 9.2$ GeV ($0 \le m_\chi \le 4.5$ GeV) by performing a series of unbinned extended maximum likelihood scans in steps of m_{A^0} (m_χ). We use two kinematic variables: the dipion recoil mass $M_{\rm recoil}$ and the missing mass squared M_X^2,

$$M_{\rm recoil}^2 = M_{\Upsilon(2S)}^2 + m_{\pi\pi}^2 - 2M_{\Upsilon(2S)}E_{\pi\pi}^*, \quad (1)$$

$$M_X^2 = (\mathcal{P}_{e^+e^-} - \mathcal{P}_{\pi\pi} - \mathcal{P}_\gamma)^2, \quad (2)$$

where $E_{\pi\pi}^*$ is the c.m. energy of the dipion system, and $\mathcal{P}$ is the four-momentum. The two-dimensional likelihood function is computed for observables $(M_{\rm recoil}, M_X^2)$ over the range $9.44 \le M_{\rm recoil} \le 9.48$ GeV and $-10 \le M_X^2 \le 68$ GeV^2 (low-mass region) and $40 \le M_X^2 \le 84.5$ GeV^2 (high-mass region). It contains contributions from signal, continuum background, radiative leptonic $\Upsilon(1S)$ background, and peaking backgrounds, as described below. We search for the A^0 in mass steps equivalent to half the mass resolution $\sigma(m_{A^0})$. We sample a total of 196 points in the low-mass $0 \le m_{A^0} \le 8$ GeV range, and 146 points in the high-mass range $7.5 \le m_{A^0} \le 9.2$ GeV. For the $\Upsilon(1S) \to \gamma\chi\bar{\chi}$ search, we use 17 values of m_χ over $0 \le m_\chi \le 4.5$ GeV. For each m_{A^0} (m_χ) value, we compute the value of the negative log-likelihood NLL $= -\ln\mathcal{L}(N_{\rm sig})$ in steps of the signal yield $N_{\rm sig} \ge 0$ while minimizing NLL with respect to the background yields $N_{\rm cont}$ (continuum), $N_{\rm lept}$ [$\Upsilon(1S) \to \gamma\ell^+\ell^-$], and, where appropriate, $N_{\rm hadr}$ (radiative hadronic background) or $N_{\eta'}$ (two-photon η' background). If the minimum of NLL occurs for $N_{\rm sig} > 0$, we compute the raw statistical significance of a particular fit as $\mathcal{S} = \sqrt{2\log(\mathcal{L}/\mathcal{L}_0)}$, where $\mathcal{L}_0$ is the value of the likelihood for $N_{\rm sig} = 0$. For small $\mathcal{S}$, we integrate $\mathcal{L}(N_{\rm sig})$ with uniform prior over $N_{\rm sig} \ge 0$ to compute the 90% C.L. Bayesian upper limits. In the range $7.5 \le m_{A^0} \le 8$ GeV and $3.5 \le m_\chi \le 4$ GeV where the low-mass and high-mass selections overlap, we add NLLs from both data sets, ignoring a small (3%) correlation. This likelihood scan procedure is designed to handle samples with a very small number of events in the signal region.

We use signal Monte Carlo samples [23,24] $\Upsilon(1S) \to \gamma A^0$ and $\Upsilon(1S) \to \gamma\chi\bar{\chi}$ generated at 17 values of m_{A^0} over a broad range $0 \le m_{A^0} \le 9.2$ GeV and at 17 values of m_χ over $0 \le m_\chi \le 4.5$ GeV to determine the signal distributions in M_X^2 and selection efficiencies. We then interpolate these distributions and efficiencies. The signal probability density function (PDF) in M_X^2 is described by a crystal ball (CB) function [25] [$\Upsilon(1S) \to \gamma A^0$] or a resolution-smeared phase-space function [$\Upsilon(1S) \to \gamma\chi\bar{\chi}$]. The resolution in M_X^2 is dominated by the photon energy resolution, and varies monotonically from 1 GeV^2 at low m_{A^0} to 0.2 GeV^2 at $m_{A^0} = 9.2$ GeV. We correct the signal PDF in M_X^2 for the difference between the photon energy resolution function in data and simulation using a high-statistics $e^+e^- \to \gamma\gamma$ sample. We determine the signal distribution in $M_{\rm recoil}$, as well as that of background containing real $\Upsilon(1S)$ decays, from a large data sample of events $\Upsilon(1S) \to \mu^+\mu^-$. This PDF is modeled as a sum of two CB functions with a common mean, a common

resolution $\sigma(M_{\rm recoil}) \approx 2$ MeV, and two opposite-side tails.

We describe the M_X^2 PDF of the radiative $\Upsilon(1S) \to \gamma\ell^+\ell^-$ background by an exponential function, and determine the exponent from a fit to the distribution of M_X^2 in a $\Upsilon(1S) \to \gamma\ell^+\ell^-$ data sample in which the two stable leptons (e or μ) are fully reconstructed. Before the fit, this sample is reweighted by the probability as a function of M_X^2 that neither lepton is observed.

The continuum M_X^2 PDF is described by a function that has a resolution-smeared phase-space component at low M_X^2, and an exponential rise at high M_X^2. For the low-mass selection ($-10 \le M_X^2 \le 68$ GeV^2), we determine this PDF from a fit to the $\Upsilon(3S)$ data sample. For the high-mass region ($40 \le M_X^2 \le 84.5$ GeV^2), we determine this PDF, as well as the M_X^2 PDF of the peaking η' background, from a fit to the $\Upsilon(2S)$ data sample selected with the NN requirement $\mathcal{N} < 0$. The $M_{\rm recoil}$ PDF is determined from a fit to the $\Upsilon(3S)$ data sample.

The contribution from the radiative hadronic backgrounds is estimated from the measurement of $\Upsilon(1S) \to \gamma h^+ h^-$ spectra [21]. We assume isospin symmetry to relate $\mathcal{B}(\Upsilon(1S) \to \gamma K^+ K^-)$ to $\mathcal{B}(\Upsilon(1S) \to \gamma K_L^0 K_L^0)$, and $\mathcal{B}(\Upsilon(1S) \to \gamma p\bar{p})$ to $\mathcal{B}(\Upsilon(1S) \to \gamma n\bar{n})$. A small additional contribution arises from $\Upsilon(1S) \to \gamma\pi^+\pi^-$ events in which the pions escape detection. We expect $N_{\rm hadr} = 6.6 \pm 1.1$ radiative hadronic events (without IFR veto), dominated by $\Upsilon(1S) \to \gamma K_L^0 K_L^0$, or $N_{\rm hadr}^{\rm veto} = 1.02 \pm 0.14$ events (with IFR veto). We describe the M_X^2 distribution of these events with a combination of CB functions, using the measured spectrum of $\Upsilon(1S) \to \gamma h^+ h^-$ events [21].

The largest systematic uncertainty is on the reconstruction efficiency, which includes the trigger or filter efficiency ($\varepsilon_{\rm trig}$), and photon (ε_γ) and dipion ($\varepsilon_{\pi\pi}$) reconstruction and selection efficiencies. We measure the product $\varepsilon_{\pi\pi} N_{\Upsilon(1S)}$, where $N_{\Upsilon(1S)}$ is the number of produced $\Upsilon(1S)$ mesons, with a clean high-statistics sample of the $\Upsilon(1S) \to \mu^+\mu^-$ decays. The uncertainty (2.1%) is dominated by $\mathcal{B}(\Upsilon(1S) \to \mu^+\mu^-)$ (2%) [3] and a small selection uncertainty for the $\mu^+\mu^-$ final state. We measure ε_γ in an $e^+e^- \to \gamma\gamma$ sample in which one of the photons converts into an e^+e^- pair in the detector material (1.8% uncertainty). The trigger efficiency $\varepsilon_{\rm trig}$ is measured in unbiased random samples of events that bypass the trigger or filter selection. This uncertainty is small for the single-photon triggers (0.4%), but is statistically limited for the dipion triggers (8%). In the low-mass region, we take into account the anticorrelation between single-photon and dipion trigger efficiencies in L3; the uncertainty for the combination of the triggers is 1.2%.

We account for additional uncertainties associated with the signal and background PDFs, and the predicted number of radiative hadronic events $N_{\rm hadr}$, including PDF parameter correlations. These uncertainties do not scale with the signal yield, but are found to be small. We also test for possible biases in the fitted value of the signal yield with a large ensemble of pseudoexperiments. The biases are consistent with zero for all values of m_{A^0} and m_χ, and we assign an uncertainty of 0.25 events.

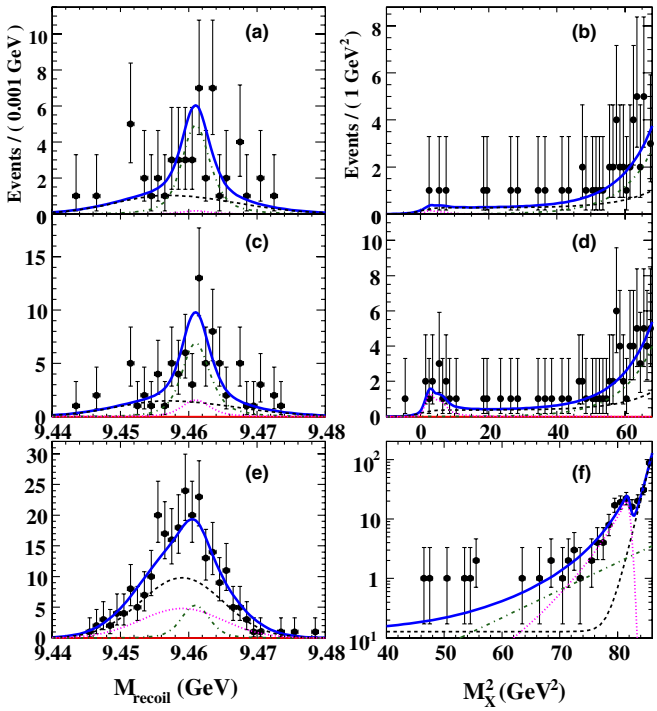

FIG. 1 (color online). Projection plots from the fit with $N_{\rm sig} = 0$ onto (a,c,e) $M_{\rm recoil}$ and (b,d,f) M_X^2. (a,b) Low-mass region with IFR veto, (c,d) low-mass region without IFR veto, (e,f) high-mass region. Overlaid is the fit with $N_{\rm sig} = 0$ (solid blue line), continuum background (black dashed line), radiative leptonic $\Upsilon(1S)$ decays (green dash-dotted line), and (c,d) radiative hadronic $\Upsilon(1S)$ decays or (e,f) η' background (magenta dotted line).

As a first step in the likelihood scan, we perform fits to the low-mass and high-mass regions with $N_{\rm sig} = 0$. The free parameters in the fit are $N_{\rm cont}$, $N_{\rm lept}$, and $N_{\rm hadr}$ (low-mass region), and $N_{\rm cont}$, $N_{\rm lept}$, and $N_{\eta'}$ (high-mass region). The results of the fits are shown in Fig. 1. We observe no significant deviations from the background-only

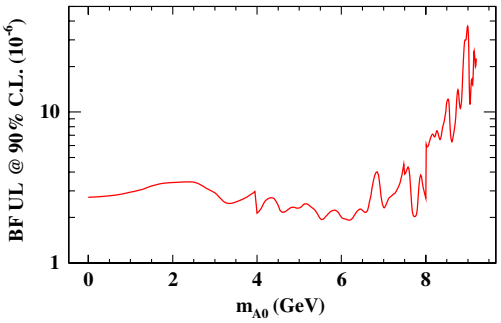

FIG. 2 (color online). Ninety percent C.L. upper limits for $\mathcal{B}(\Upsilon(1S) \to \gamma A^0) \times \mathcal{B}(A^0 \to \text{invisible})$.

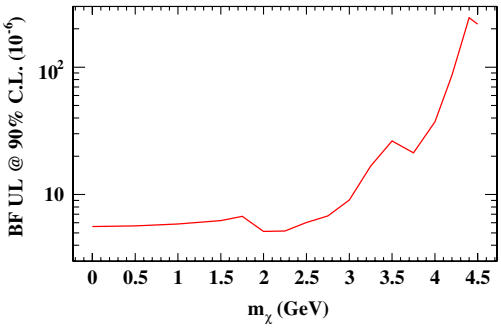

FIG. 3 (color online). Ninety percent C.L. upper limits for $\mathcal{B}(\Upsilon(1S) \to \gamma\chi\bar{\chi})$.

hypothesis. We find $N_{\rm hadr} = 8.7^{+4.0}_{-3.3} \pm 0.8$ (without IFR veto) with a significance of 3.5σ, including systematic uncertainties.

We then proceed to perform the likelihood scans as a function of $N_{\rm sig}$ in steps of m_{A^0} and m_χ. In the scan, the contribution of the radiative hadronic background is fixed to the expectation $N_{\rm hadr} = 1.02 \pm 0.14$ for $m_{A^0} < 4$ GeV ($m_\chi < 2$ GeV) where the IFR veto is applied, and to $N_{\rm hadr} = 6.6 \pm 1.1$ for fits in the $4 \le m_{A^0} \le 8$ GeV ($2 \le m_\chi < 4$ GeV) range. We do not observe a significant excess of events above the background, and set upper limits on $\mathcal{B}(\Upsilon(1S) \to \gamma A^0) \times \mathcal{B}(A^0 \to \text{invisible})$ (Fig. 2) and $\mathcal{B}(\Upsilon(1S) \to \gamma\chi\bar{\chi})$ (Fig. 3). The limits are dominated by statistical uncertainties. The largest statistical fluctuation, 2.0σ, is observed at $m_{A^0} = 7.58$ GeV [26]; we estimate the probability to see such a fluctuation *anywhere* in our data set to be over 30%.

In summary, we find no evidence for the single-photon decays $\Upsilon(1S) \to \gamma + \text{invisible}$, and set 90% C.L. upper limits on $\mathcal{B}(\Upsilon(1S) \to \gamma A^0) \times \mathcal{B}(A^0 \to \text{invisible})$ in the range $(1.9\text{–}4.5) \times 10^{-6}$ for $0 \le m_{A^0} \le 8.0$ GeV, $(2.7\text{–}37) \times 10^{-6}$ for $8 \le m_{A^0} \le 9.2$ GeV, and scalar A^0. We limit $\mathcal{B}(\Upsilon(1S) \to \gamma\chi\bar{\chi})$ in the range $(0.5\text{–}24) \times 10^{-5}$ at 90% C.L. for $0 \le m_\chi \le 4.5$ GeV, assuming the phase-space distribution of photons in this final state. Our results improve the existing limits by an order of magnitude or more, and significantly constrain [26] light Higgs boson [13] and light dark matter [8] models.

We are grateful for the excellent luminosity and machine conditions provided by our PEP-II colleagues, and for the substantial dedicated effort from the computing organizations that support *BABAR*. The collaborating institutions wish to thank SLAC for its support and kind hospitality. This work is supported by DOE and NSF (USA), NSERC (Canada), CEA and CNRS-IN2P3 (France), BMBF and DFG (Germany), INFN (Italy), FOM (The Netherlands), NFR (Norway), MES (Russia), MICIIN (Spain), STFC (United Kingdom). Individuals have received support from the Marie Curie EIF (European Union), the A. P. Sloan Foundation (USA), and the Binational Science Foundation (USA-Israel).

*Now at Temple University, Philadelphia, PA 19122, USA.
†Also with Dipartimento di Fisica, Università di Perugia, Perugia, Italy.
‡Also with Università di Roma La Sapienza, I-00185 Roma, Italy.
§Now at University of South Alabama, Mobile, AL 36688, USA.
‖Also with Università di Sassari, Sassari, Italy.

[1] E. Komatsu *et al.* (WMAP Collaboration), Astrophys. J. Suppl. Ser. **180**, 330 (2009); M. Tegmark *et al.* (SDSS Collaboration), Phys. Rev. D **74**, 123507 (2006).
[2] G. Bertone, D. Hooper, and J. Silk, Phys. Rep. **405**, 279 (2005).
[3] K. Nakamura *et al.* (Particle Data Group), J. Phys. G **37**, 075021 (2010).
[4] J. F. Gunion, D. Hooper, and B. McElrath, Phys. Rev. D **73**, 015011 (2006).
[5] P. Jean *et al.*, Astron. Astrophys. **407**, L55 (2003); J. Knodlseder *et al.*, Astron. Astrophys. **411**, L457 (2003).
[6] R. Bernabei *et al.* (DAMA Collaboration), Eur. Phys. J. C **56**, 333 (2008).
[7] B. Aubert *et al.* (*BABAR* Collaboration), Phys. Rev. Lett. **103**, 251801 (2009).
[8] G. K. Yeghiyan, Phys. Rev. D **80**, 115019 (2009).
[9] R. McElrath, in *Proceedings of the CHARM 2007 Workshop, Ithaca, NY, 2007*, econf C070805, 19 (2007) (arXiv:0712.0016); P. Fayet, Phys. Rev. D **81**, 054025 (2010).
[10] F. Wilczek, Phys. Rev. Lett. **39**, 1304 (1977).
[11] R. Dermisek and J. F. Gunion, Phys. Rev. Lett. **95**, 041801 (2005).
[12] M. Lisanti and J. G. Wacker, Phys. Rev. D **79**, 115006 (2009).
[13] R. Dermisek, J. F. Gunion, and B. McElrath, Phys. Rev. D **76**, 051105 (2007); R. Dermisek and J. F. Gunion, Phys. Rev. D **81**, 075003 (2010).
[14] R. E. Shrock and M. Suzuki, Phys. Lett. **110B**, 250 (1982).
[15] R. Balest *et al.* (CLEO Collaboration), Phys. Rev. D **51**, 2053 (1995).
[16] E. Fullana and M. A. Sanchis-Lozano, Phys. Lett. B **653**, 67 (2007).
[17] B. Aubert *et al.* (*BABAR* Collaboration), Nucl. Instrum. Methods Phys. Res., Sect. A **479**, 1 (2002).
[18] W. Menges, IEEE Nucl. Sci. Symp. Conf. Rec. **5**, 1470 (2006).
[19] Henceforth, $*$ marks c.m. quantities.
[20] A. Höcker *et al.*, Proc. Sci., ACAT (2007) 040; http://tmva.sourceforge.net/.
[21] S. B. Athar *et al.* (CLEO Collaboration), Phys. Rev. D **73**, 032001 (2006).
[22] G. Punzi, arXiv:physics/0308063.
[23] S. Agostinelli *et al.* (GEANT4 Collaboration), Nucl. Instrum. Methods Phys. Res., Sect. A **506**, 250 (2003).
[24] D. Lange, Nucl. Instrum. Methods Phys. Res., Sect. A **462**, 152 (2001).
[25] M. J. Oreglia, Ph.D. thesis [Report No. SLAC-236, 1980], Appendix D.
[26] See supplemental material at http://link.aps.org/supplemental/10.1103/PhysRevLett.107.021804 for additional plots.